Journal of the Physical Society of Japan
Vol. 68, No. 4, April, 1999, pp. 1398-1403

Symmetry Analysis of the Fermi Surface States of Sr_2RuO_4 by Display-Type Photoelectron Spectroscopy

Taichi OKUDA*, Masato KOTSUGI, Kan NAKATSUJI, Masao FUJIKAWA, Shigemasa SUGA, Yasuhisa TEZUKA[1], Shik SHIN[1], Masahiro KASAI[2], Yoshinori TOKURA[3] and Hiroshi DAIMON[4]

Department of Material Physics, Faculty of Engineering Science, Osaka University, Toyonaka, Osaka 560-8531
[1]*Institute for Solid State Physics, The University of Tokyo, Tanashi, Tokyo 188-0002*
[2]*Joint Research Center of Atom Technology (JRCAT), Tsukuba, Ibaraki 305-0046*
[3]*Department of Applied Physics, Faculty of Engineering, The University of Tokyo, Bunkyo-ku, Tokyo 113-8656*
[4]*Graduate School of Materials Science, Nara Institute of Science and Technology, Ikoma, Nara 630-0101*

(Received November 16, 1998)

The Fermi surface of the noncuprate superconductor Sr_2RuO_4 has been studied in detail by two-dimensional angle resolved photoelectron spectroscopy (2D-ARPES) using a display-type electron spectrometer and a linearly polarized synchrotron radiation. The existence of the large Fermi surfaces agrees with previous band calculations and conventional ARPES measurements. From the comparison of the observed photoelectron intensity distribution of the Fermi surface with that of the simulation for atomic orbitals, the symmetry of the atomic orbitals composing the Fermi surfaces is revealed to be the $d\varepsilon$;d_{xy}, d_{yz}, d_{zx}-like in contrast to the $d_{x^2-y^2}$-like orbital in the cuprate high-T_c super conductor. The possibility of the existence of the extended van-Hove singularity just below the Fermi level, which was suggested by recent conventional ARPES measurements, is also discussed.

KEYWORDS: Fermi surface, superconductor, photoelectron angular distribution, two-dimensional angle resolved photoemission, van Hove singularity

§1. Introduction

Since the discovery of the high T_c cuprate superconductors (abbreviated as HTSC hereafter), various efforts have been made to investigate their electronic structure in the normal and superconducting phases. The noncuprate superconductor Sr_2RuO_4 gives a unique opportunity to investigate the role of the two-dimensionality and has been studied intensively. This Sr_2RuO_4, the noncuprate oxide superconductor[1] with low $T_c \sim 0.93$ K, has the same crystal structure as the La_2CuO_4 (K_2NiF_4 structure) which is the parent material of the HTSCs. In contrast to the $3d^9$ state of Cu 2^+ in La_2CuO_4,[2] Ru is 4^+ in Sr_2RuO_4 and has the $4d^4$ state. Oguchi[3] and Singh[4] have calculated the band structure of Sr_2RuO_4 independently, using the local-density approximation (LDA) of the linearized augmented plane-wave (LAPW) method. According to their band calculations three bands hybridized between the Ru $4d$ and O $2p$ states cross the Fermi level and make large Fermi surface. It is predicted that the antibonding state between the Ru $4d$ d_{xy}, d_{yz}, d_{zx} and O $2p\pi$ orbitals contributes to the Fermi surface in contrast to the case of the HTSC whose Fermi surface is considered to be formed of the Cu $3d_{x^2-y^2}$ and O$2p$ σ antibonding state. The Ru $4d$ orbitals are extended and hybridized with the O $2p$ state, leading to the large ligand field splitting.

Conventional angle resolved photoelectron spectroscopy (ARPES) studies of Sr_2RuO_4 with high energy resolution ($\sim$50 meV) have been reported by two different groups.[5,6] From the ARPES measurements both groups have independently reported the existence of the extended van-Hove singularity (evHs) just below the Fermi level (11[5]$\sim$16 meV[6]) which is considered to be one of the most important feature of the HTSC. According to the band calculations, however, the vHs is predicted above the Fermi level ($E_B = -250$ meV[3] and -60 meV & -260 meV[4]).

As for the Fermi surface topology both the band calculations[3,4] and the ARPES measurements[5,6] suggest the existence of large Fermi surfaces. The Fermi surface obtained by the ARPES measurements[5,6] is, however, interpreted to consist of two hole and one electron bands, in contrast to the results of band calculations[3,4] which predict one hole and two electron bands. On the other hand, the results of de Haas-van Alphen oscillation[7] is consistent with the band calculations.

In this paper we report the results of the direct observation of the Fermi surfaces of Sr_2RuO_4 by two-dimensional ARPES (2D-ARPES) measurement using a display-type electron spectrometer and a linearly polarized synchrotron radiation (SR). The obtained Fermi surface topology is compared with that of the band calculation[3] and the conventional ARPES measurement.[5] From the dependence of the photoelectron angular distribution (PEAD) pattern at the Fermi level on polarization of the excitation light, we conclude that the Fermi surface consists dominantly of the Ru $4d\varepsilon$ orbital as expected by the band calculations.[3,4] The possibility of existence of the evHs is also discussed from the obtained

* Present address: The Institute of Physical and Chemical Research (RIKEN), Saitama 351-0198, Japan. E-mail: okudat@postman.riken.go.jp

PEAD patterns of the Fermi surface.

§2. Experimental

The PEAD patterns have been measured using a two-dimensional display-type hemispherical mirror analyzer,[8] which was installed at the beam-line BL-4 of SOR-RING in the Synchrotron Radiation Laboratory of Institute for Solid State Physics (SRL-ISSP), The University of Tokyo. This analyzer can simultaneously detect all photoelectrons emitted within ±60° polar angles from the surface normal for 360° azimuthal angles. The Sr_2RuO_4 single crystal was grown by a floating zone method. The clean surface was obtained by cleaving the sample in an ultra-high vacuum (UHV) chamber and the surface quality was checked by low energy electron diffraction (LEED). The base pressure of the measurement chamber was less than 1.5×10^{-10} Torr. The sample was cooled down to about 150 K by liquid nitrogen during the sample cleavage and ARPES measurement. To avoid the contamination effect a series of the measurements was done within 6 hours after the cleavage. Especially the PEAD patterns of the Fermi surface were recorded in less than 2 hours after cleaving. The linearly polarized excitation light was incident to the sample normal direction (i.e. along the c axis; the light was s-polarized). We have measured the PEAD patterns in two different configurations, one with the electric vector $\boldsymbol{E}$ of SR-light parallel to the vector **a** (=**b**) of the sample (we call this configuration as 0° configuration) and the other with the $\boldsymbol{E}$ parallel to the vector of **a** + **b** (45° configuration). The photoelectrons were detected as light pulses on the phosphorescence screen after being intensified by double micro-channel plates. The PEAD patterns on the phosphorescence screen were measured through a view port by a commercial CCD camera which was set outside the UHV chamber. The typical measurement time of each PEAD pattern was about 10~30 min. The energy and angular resolutions of the measurement were about $\Delta E = 250$ meV and $\Delta(\theta, \phi) = \pm2°$, respectively.

§3. Results

Figure 1 shows a photoemission spectrum of Sr_2RuO_4 which was recorded with the angle integrated mode at $h\nu = 30$ eV using aforementioned display-type analyzer,[8] compared with the total density of states (DOS) calculated by Oguchi.[3] The positions of the prominent peaks labeled as A, B, C and D agree well with those observed by Schmidt *et al.*[9] and Inoue *et al.*[10] by angle integrated photoelectron spectroscopy at $h\nu = 60$ and 110 eV[9] and 21.2 eV.[10] We also labeled prominent peaks of calculated DOS as A′, B′, C′ and D′ considering the correspondence with experimental ones. According to the band calculations,[3,4] the state A′ crossing the Fermi level consists of the antibonding state between the Ru $4d\varepsilon$ (d_{xy}, d_{yz}, d_{zx}) and O $2p\pi$ orbitals. Other structures C′ and D′ are the Ru $4d\varepsilon$-O $2p\pi$ bonding states. The structure B′ is a non-bonding O $2p$ state. The band widths of these structures can roughly explain the widths of the observed photoemission spectrum. In

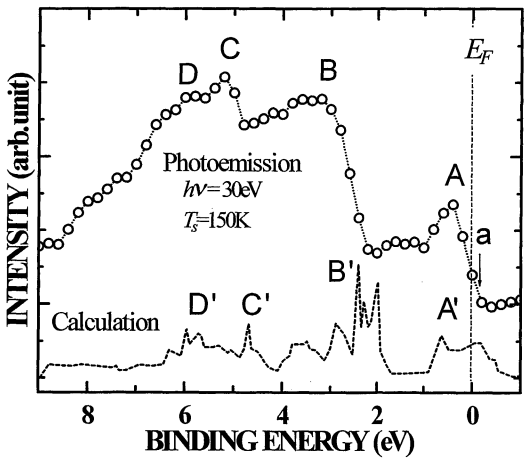

Fig. 1. Angle integrated valence band photoemission spectrum of Sr_2RuO_4 measured at $h\nu = 30$ eV and 150 K, compared with the density of state of Sr_2RuO_4 calculated by Oguchi.[3]

a strict sense, the shape of the experimental spectrum, however, is quite different from that of the calculation. These discrepancies of the binding energy (E_B) and the spectral weight between photoemission and the calculation have been discussed by Inoue *et al.*[10] as the effect of strong electron correlation in the system.

We measured the PEAD patterns of the Fermi level states in two different configurations as illustrated at the top of Fig. 2. In the illustration, filled and open circles represent the Ru and O atoms in the Ru-O plane. The broken arrows show the direction of the electric vector $\boldsymbol{E}$ of the incident light. The 0° configuration means that $\boldsymbol{E}$ is parallel to the Ru-O bonding direction ($\bar{\Gamma}$-$\bar{Z}$ direction in the Brillouin zone) and the 45° configuration means that $\boldsymbol{E}$ is 45° from the Ru-O bonding direction ($\bar{\Gamma}$-$\bar{X}$ direction). For the PEAD pattern of Fermi surface, we measured the patterns at E_B of −0.1 eV represented by a in Fig. 1 by considering the finite energy resolution ($\Delta E \sim 250$ meV). By setting the central detection energy just above the Fermi level and utilizing the tail of the window function, we can realize higher energy resolution (~100 meV) than the nominal energy resolution.

Figures 2(A) and 2(B) are the PEAD patterns observed in the aforementioned two different configurations ((A) 0° configuration and (B) 45° configuration). These PEAD patterns were symmetrized by two mirror planes considering the symmetry of the sample, after dividing the images by the analyzer transmittance pattern. In these figures the brighter region corresponds to the region where the photoelectron intensity is higher. There is a low-efficient region in the micro-channel plate where the incident direction of the electrons on it is rather parallel to the channel. The dark spots around the center of Figs. 2(A) and 2(B) correspond to this low-efficient region multiplied by the above mentioned symmetry operation. The white lines are boundaries of the Brillouin Zone (BZ) which were drawn afterward. The symmetry points, $\bar{\Gamma}$, $\bar{X}$, $\bar{M}$ and $\bar{Z}$ (abbreviated as Γ, X, M and Z in the figure) are also indicated. The bright regions of the PEAD patterns of both 0° and 45° configurations are observed mainly inside the 1st BZ, and the photoemis-

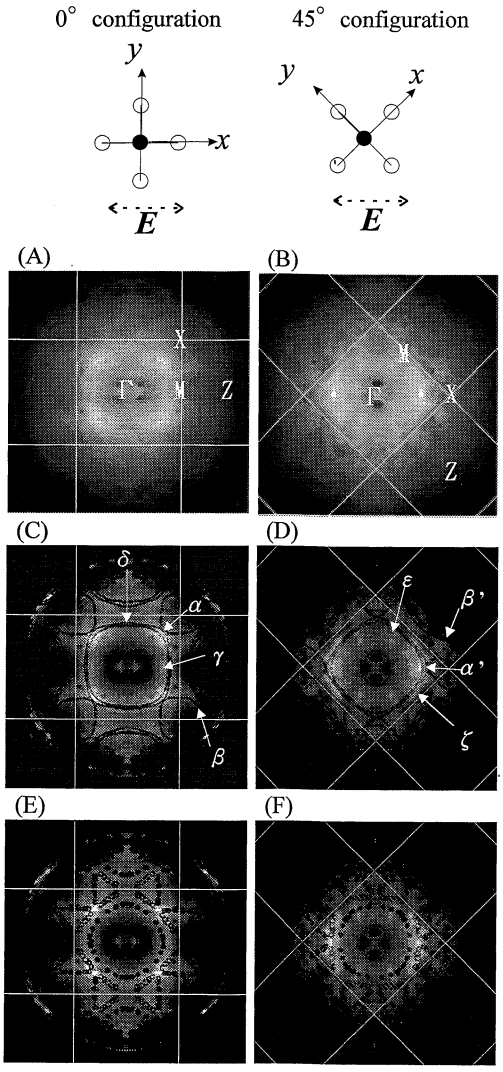

Fig. 2. Photoelectron angular distribution (PEAD) pattern of the Fermi surface of Sr_2RuO_4 measured by a display-type analyzer (A) in the 0° configuration and (B) in the 45° configuration. Illustrations at the top show the two different measurement configurations. Filled and open circles represent the Ru and O atoms in Ru-O plane, and the broken arrow shows the direction of the electric vector of the incident light. The brighter region in the PEAD patterns indicates the stronger intensity of photoelectron. The boundaries of the Brillouin zone (BZ) and the symmetry points, Γ, X, M and Z are also indicated in (A) and (B). In (C) and (D), we adjusted the photoemission intensity considering the effect of the photoelectron surface escape probability and added the calculated Fermi surfaces (=solid curves) by Oguchi.[3] We labeled α, β, γ, δ, α', β', ϵ and ζ for the prominent structures of the observed Fermi surface for clarity. In (E) and (F), we also superimposed the estimated Fermi surface by conventional ARPES measurement (filled and open circles) by Yokoya *et al.*[5] on the PEAD patterns for comparison.

sion intensity is relatively weak at higher polar angles. The reduction of the photoemission intensity at higher polar angles may be caused by the reduction of the escape probability of the photoelectrons from the surface at higher polar angles. Thus we corrected the intensity in the periphery by dividing the pattern by $a_0 \cos\theta + b_0$ fitted to the background of the observed patterns. Then we can more clearly grasp the features of the observed patterns (Figs. 2(C) and 2(D)). We labeled α, β, γ, δ, α', β', ϵ and ζ for these prominent features in Figs. 2(C) and 2(D). From the shapes and positions in BZ of these peaks we consider that the α and α', and the β and β' are originated from the same band, respectively.

As shown in the PEAD pattern of the 0° configuration in Fig. 2(C), brighter regions, α, appear near the four corners of the BZ boundary having a center of gravity at about 2/3 of the $\bar{\Gamma}$-$\bar{X}$ line. These bright regions are accompanied with weaker structures, β, which surround the $\bar{X}$ points. In addition, it is seen that dark regions surround the $\bar{\Gamma}$ point. However, the sharp dark regions near the $\bar{\Gamma}$ point are rather artificial as pointed out already. Around the $\bar{\Gamma}$ point some weak structures labeled γ and δ are also seen.

In contrast to the PEAD pattern of the 0° configuration with four bright regions (α) near the corners of the BZ boundary, that of the 45° configuration (Fig. 2(D)) has two bright regions, α', near the corners at the same wave vector as that of the 0° configuration. The centers of these bright regions are along the $\bar{\Gamma}$-$\bar{X}$ line parallel to $\boldsymbol{E}$. The photoelectron intensities are suppressed along the other $\bar{\Gamma}$-$\bar{X}$ line perpendicular to $\boldsymbol{E}$ and there are no bright regions near the upper and lower corners of the BZ boundary. This intensity reduction is thought to result from the selection rule of the dipole transition as discussed afterward. The two bright regions are accompanied with weak structures, β', which surround the $\bar{X}$ points as in the case of the 0° configuration. In addition to these structures some weak and complex structures (for example ϵ or ζ) are also seen in the PEAD pattern of the 45° configuration.

§4. Discussion

The PEAD pattern is considered to be a product of the one-dimensional density of states (1D-DOS resulting from the band structure), photoemission structure factor (PSF), and angular distribution from atomic orbital (ADAO).[11] Although PSF and ADAO modify the intensity, it is considered that observation of clear intensity strongly suggests the presence of the Fermi surface in that region. In Figs. 2(C) and 2(D), we added the calculated Fermi surfaces[3] by solid curves on our corrected experimental results. Comparing the calculated results with our experimental ones, the gross shape of the Fermi surface and the existence of the large Fermi surfaces are generally consistent. In terms of the calculated Fermi surface, the strong intensity regions, α and α', are ascribed to the three Fermi surfaces approaching to each other. However, we could not obtain any direct proof of the existence of two electronic Fermi surfaces predicted by the calculations.[3,4] The results of the de Haas-van Alphen experiment[7] have suggested that the Fermi surface is composed of two large electron and one narrow hole cylinders in consistent with the band calculations.[3,4] According to the recent conventional ARPES measurements reported by Yokoya *et al.*[5] and Lu *et al.*,[6] however, the experimentally derived Fermi surface is composed of one electron and two hole Fermi surfaces in contrast to the band calculation. In Figs. 2(E) and 2(F) we also compare the results of the conventional ARPES measurement[5] (one electron and two hole Fermi surfaces represented by the full and empty circles with our re-

sults). It is shown that the electron Fermi surface probed by the photoemission measurement is smaller than that of the band calculation as seen in both Figs. 2(D) and 2(F). Even in Fig. 2(E), the boundary where the photoemission intensity reduces drastically to zero around the $\bar{\Gamma}$ point in our PEAD pattern seems to be consistent with the smaller electron Fermi surface in their size and shape. In addition, the state corresponding to the region ζ, which spreads from the brightest area to the $\bar{M}$ point in Fig. 2(D) is similar to the controversial hole Fermi surface suggested by the conventional ARPES measurement. In order to more accurately investigate the Fermi surface shape, however, it is necessary to perform the measurement in higher angular and energy resolutions.

2D-ARPES measurement is also useful to investigate the symmetry of the atomic orbital composing the Fermi surfaces. The observed PEAD pattern is necessarily influenced by the ADAO effect which reflects the atomic orbital character of the initial state as well as by the PSF effect, which reflects the details of the wave-function of the band. In other words, the photoemission intensity is suppressed in the wave vector region with small ADAO factor caused by the dipole selection rule for atomic orbitals, even if corresponding electronic state (=band) exists. Thus we can qualitatively discuss the character of the atomic orbitals which contribute to the Fermi surfaces from the comparison of the observed PEAD patterns with ADAO pattern.

Figures 3(a) to 3(j) show the calculated ADAO patterns of the atomic d orbitals (d_{xy}, d_{yz}, d_{zx}, $d_{x^2-y^2}$ and d_{z^2}) for the 0° and 45° configurations. These patterns are the photoemission intensity distribution from each atomic orbital. The transition probabilities of them are calculated by considering the spherical harmonics of the atomic orbital in the initial state, the plane wave of free electron as the final state, and the linearly polarized light as the incident light. The periphery of the circle of these patterns corresponds to the polar angle of 60°, and the squares and diamonds show the size of the 1st BZ in the 0° and 45° configurations at the incident photon energy of 30 eV. In accordance with the dipole selection rule restricted by the symmetry of each atomic orbital and the electric field of the incident light, each d orbital shows characteristic ADAO pattern. The d_{xy} orbital in the measurement of the 45° configuration (=(f) $d_{xy}^{45^\circ}$) gives the same pattern as the $d_{x^2-y^2}$ orbital in the 0° configuration ((d) $d_{x^2-y^2}^{0^\circ}$) and *vice versa* (i.e. (a) $d_{xy}^{0^\circ}$=(i) $d_{x^2-y^2}^{45^\circ}$). The symmetry does not change in the 0° and 45° configuration for the d_{z^2} orbital ((e) $d_{z^2}^{0^\circ}$=(j) $d_{z^2}^{45^\circ}$).

From the numerous studies of the cuprate HTSC, it is believed that the Fermi surface of the HTSC consists of the Cu3d $d_{x^2-y^2}$-O2$p\sigma$ antibonding state.[12] If the atomic orbitals composing the Fermi surface of Sr_2RuO_4 have the same symmetry as those of the HTSC, the intensity of the whole PEAD pattern should be modified by the ADAO patterns of Figs. 3(d) ($d_{x^2-y^2}^{0^\circ}$) and 3(i) ($d_{x^2-y^2}^{45^\circ}$) in the measurements of the 0° and 45° configurations, respectively. In Fig. 2(D), however, the intensity of the Fermi surface along the direction perpendicular to $\boldsymbol{E}$ is suppressed compared to the strong intensities, α', parallel to $\boldsymbol{E}$. This distribution of the photoelectron intensity is evidently different from Fig. 3(i) ($d_{x^2-y^2}^{45^\circ}$) which has strong (weak) intensity region perpendicular (parallel) to $\boldsymbol{E}$. Thus the Fermi surface of Sr_2RuO_4 does not have the $d_{x^2-y^2}$ symmetry in contrast to the HTSCs.

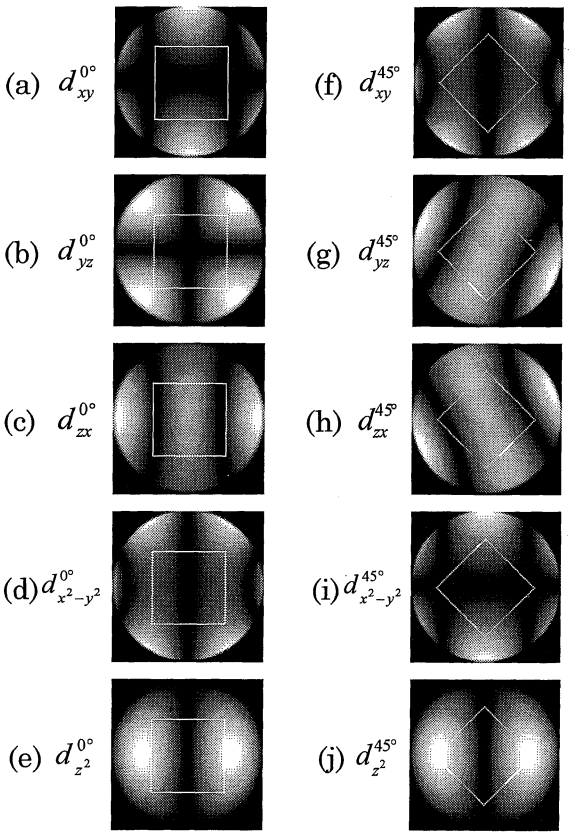

Fig. 3. The calculated patterns of angular distribution of atomic orbitals (ADAO) of (a) $d_{xy}^{0^\circ}$, (b) $d_{yz}^{0^\circ}$, (c) $d_{zx}^{0^\circ}$, (d) $d_{x^2-y^2}^{0^\circ}$, (e) $d_{z^2}^{0^\circ}$, (f) $d_{xy}^{45^\circ}$, (g) $d_{yz}^{45^\circ}$, (h) $d_{zx}^{45^\circ}$, (i) $d_{x^2-y^2}^{45^\circ}$, and (j) $d_{z^2}^{45^\circ}$ Squares and diamonds in (a) to (j) show the sizes of the 1st BZ of 0° and 45° configurations at $h\nu = 30$ eV, respectively.

According to the band calculations,[3,4] the Fermi surface of Sr_2RuO_4 is dominantly composed of the Ru 4$d\varepsilon$ (=d_{xy}, d_{yz}, and d_{zx}) orbitals. The band calculation[3] predicted that the antibonding d_{yz}-$p\pi$ (d_{zx}-$p\pi$) band is *fully occupied* on the $\bar{\Gamma}$-$\bar{M}$-$\bar{Z}$ line (=Δ line) along the x (y) direction in Fig. 2. That is, the Fermi surface along the Δ line consists of the d_{xy} and d_{zx} states (d_{xy} and d_{yz} states) along the $x(y)$ direction. Meanwhile, on the $\bar{\Gamma}$-$\bar{X}$ line, every $d\varepsilon$ state, d_{xy}, d_{yz}, and d_{zx}, crosses the Fermi level and forms the Fermi surface. On the basis of this prediction of the band calculation, the bright areas, α and α', observed near the corners of the 1st BZ of Figs. 2(C) and 2(D) correspond to the triply gathering Fermi surfaces of d_{xy}, d_{yz} and d_{zx} orbitals. On the other hand the weaker intensity in the region of γ (δ) in Fig. 2(C), on the Δ line along the $x(y)$ direction can be the contribution of the d_{xy} and d_{zx} (d_{xy} and d_{yz}) orbitals.

Comparing the PEAD patterns in the 0° configuration (Fig. 2(C)) with the simulated ADAO patterns of $d\varepsilon$ (Figs. 3(a) d_{xy}, 3(b) d_{yz} and 3(c) d_{zx}), one can recognize the following correspondence. That is, the four bright areas, α, in Fig. 2(C) are consistent with the bright areas

of $d_{yz}^{0°}$ pattern in Fig. 3(b). Other $d\varepsilon$ states(Fig. 3(a) $d_{xy}^{0°}$ and 3(c) $d_{zx}^{0°}$), less contribute to the intensity in the area α, because of their intensity suppression in the corresponding region by the ADAO effect, even if the corresponding band contains those d_{xy} and d_{zx} components. As already mentioned for the PEAD pattern of (D) in the 45° configuration, on the other hand the bright areas at the corners are suppressed along the direction perpendicular to the electric field $\boldsymbol{E}$ and only two bright areas labeled α' remain. This suppression of the photoelectron intensity is consistent only with the ADAO pattern of $d_{xy}^{45°}$ in Fig. 3(f). Assuming that the Fermi surface consists of only $d\varepsilon$ states, this result suggests that the d_{xy} orbital contributes dominantly to the Fermi surface in the region of α'. Comparing the ADAO pattern of d_{z^2} in Figs. 3(e) and 3(j) with the PEAD patterns of (C) and (D), its ADAO pattern is also consistent with the intensity change of α and α'. According to the band calculation, the d_{z^2} band has small dispersion along the k_z direction and small amount of the d_{z^2} orbital can contribute the Fermi surface at certain k_z value.[13] Therefore the d_{z^2} orbital can contribute also to the Fermi surface and we cannot exclude the contribution of the d_{z^2} orbital to the α and α' states from our experimental results alone. However, considering the relatively higher energy position of the d_{z^2} orbital than that of the $d\varepsilon$ orbitals on account of the influence of the crystal field, it is not likely that the d_{z^2} orbital contributes dominantly to the Fermi surface of Sr_2RuO_4. As for the intensities around the $\bar{X}$ point, β and β' are compatible with the ADAO of $d_{yz}^{0°}$ in Fig. 3(b) and $d_{xy}^{45°}$ in Fig. 3(f). The intensity in the region of β' is unclear near the upper and lower $\bar{X}$ points located perpendicularly to the $\boldsymbol{E}$ in Fig. 2(D). This is consistent with the Fig. 3(f) ($d_{xy}^{45°}$).

The weak but appreciable intensities, δ, in the upper and lower parts in Fig. 2(C) are compatible with the bright areas of $d_{xy}^{0°}$ in Fig. 3(a) and $d_{zx}^{0°}$ in Fig. 3(c). The weak intensities, in the regions ζ and ϵ near the $\bar{M}$ points in the PEAD pattern of 45° configuration, can be contributed by the ADAO of Figs. 3(f) $d_{xy}^{45°}$, 3(g) $d_{yz}^{45°}$, and 3(h) $d_{zx}^{45°}$ as well as (e) d_{z^2}. The intensity γ, in (C), however, cannot be explained by the contribution of the ADAO patterns of any $d\varepsilon$ orbitals in the 0° configuration (Figs. 3(a)–3(c)). As mentioned above, small amount of the d_{z^2} orbital can contribute the Fermi surface and the weak intensities in the region of γ may suggest the weak contribution of the d_{z^2} orbital to the Fermi surface along the Δ line.

As mentioned above, it is confirmed that the Fermi surface of Sr_2RuO_4 is composed of the d_{xy}, d_{yz}, and d_{zx} orbitals rather than the $d_{x^2-y^2}$ orbital, being consistent with the band calculations.[3,4] This experimental result is also consistent with the recently reported symmetry observation of the unoccupied state of Sr_2RuO_4 by angle resolved x-ray absorption extended fine structure (EXAFS) study by Schmidt *et al.*,[9] in which they assign the peaks of the EXAFS spectra consistently with the prediction of the band calculations.[3,4]

Aforementioned conventional ARPES measurements with high energy resolution (~50 meV)[5,6] have offered another important suggestion that there is evHs

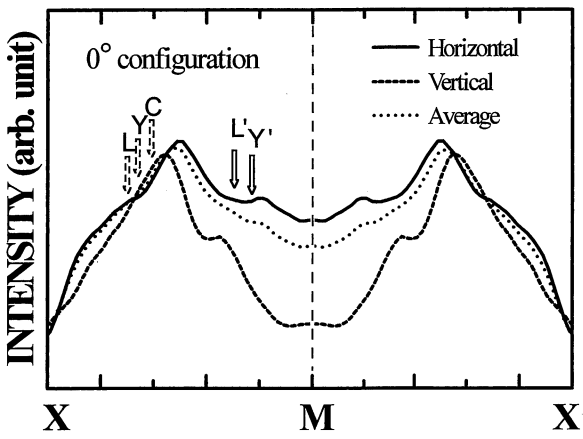

Fig. 4. Intensity profiles of the PEAD pattern of Fig. 2(C) in the 0° configuration along the $\bar{X}$-$\bar{M}$-$\bar{X}$ line. Horizontal and vertical profiles to the electric vector ($\boldsymbol{E}$ in Fig. 2) and their average are indicated by solid, dashed and dotted curves. The crossing point of the hole Fermi surface around $\bar{X}$ calculated by Oguchi[3] or Singh,[4] as well as those observed by conventional ARPES measurements by Yokoya *et al.*[5] and Lu *et al.*[6] are indicated by broken arrows labeled C, Y and L. Arrows labeled Y′ and L′ are also the crossing points of the other hole Fermi surface reported by Yokoya *et al.*[5] and Lu *et al.*,[6] respectively.

in Sr_2RuO_4 near the $\bar{M}$ point at E_B of about 11 meV[5]~16 meV.[6] The evHs state at the $\bar{M}$ point provides appreciable photoelectron intensity at the $\bar{M}$ point. On the other hand the band calculations predict that the vHs is located *above* E_F at about 250 meV[3] or 60 and 260 meV,[4] respectively. These results of the calculations mean that there is no state at the $\bar{M}$ point which corresponds to the photoemission intensity observed by the conventional ARPES measurements. The evHs just *below* the Fermi level is considered to be one of the most important features of the HTSC. If Sr_2RuO_4 with low T_c has also the similar evHs just below the Fermi level as suggested by the conventional ARPES measurements,[5,6] one has to reconsider the validity of the relationship between the existence of the evHs and the HTSC.

Direct determination of the E_B of the evHs state is impossible in our measurement because of the finite energy resolution of our display-type analyzer. But if there were evHs near the $\bar{M}$ point just below the Fermi level, high intensity in the corresponding region should be observed in our PEAD pattern. Figure 4 shows the intensity profile of the PEAD pattern along the $\bar{X}$-$\bar{M}$-$\bar{X}$ direction of the 0° configuration after background subtraction (corresponding to PEAD pattern Fig. 2(C)). Profiles along the horizontal (solid curve) and vertical (dashed curve) lines as well as their average (dotted curve) are presented. The position of the peaks of the profile is considered to be the crossing point of the Fermi surface surrounding the $\bar{X}$ point. The wave vector of the peak positions ($0.51\overline{MX}$ and $0.55\overline{MX}$ for horizontal and vertical $\bar{X}$-$\bar{M}$-$\bar{X}$ lines, respectively) agrees reasonably with that of the calculated Fermi surface by Oguchi or Singh ($0.61\overline{MX}$; indicated by a broken arrow labeled C). Those observed by conventional ARPES measurements[5,6] are indicated by Y and L ($0.63\overline{MX}$[5] and $0.65\overline{MX}$,[6] respectively) which are

a little closer to the $\bar{X}$ point than our result.

In the vertical profile the intensity at the $\bar{M}$ point is much lower than that at the peak corresponding to the Fermi surface. On the other hand, the horizontal profile is relatively shallow around the $\bar{M}$ point. This relatively high intensity around the $\bar{M}$ point in the horizontal profile suggests the existence of the photoemission intensity at $\bar{M}$ point and may indicate the existence of the evHs. Since the evHs state originate from the band forming the Fermi surface, the symmetry of the atomic orbitals of the evHs state is also considered to be the $d\varepsilon$ orbital. The higher intensity in the horizontal profile than in the vertical one, suggests that the state should be $d^{0^\circ}_{xy}$ or $d^{0^\circ}_{zx}$ or both of them being consistent with the symmetry of the atomic orbitals consisting the Fermi surface. In addition, the shoulder of the vertical profile can be assigned as the appearance of the other hole Fermi surface which is observed by Yokoya *et al.* or Lu *et al.* at the positions indicated by arrows labeled Y′ and L′. However, we have to be careful to conclude the observation of evHs because of our finite angular resolution.

§5. Conclusion

We have performed two-dimensional angle resolved photoelectron spectroscopy on the noncuprate superconductor Sr_2RuO_4 by using a display-type hemispherical mirror analyzer. Directly observed shape of the Fermi surface was compared with the results of the band calculation and the conventional ARPES measurement. The existence of the large Fermi surface is consistent with the band calculation, the ARPES measurement and the de Haas van Alphen oscillation. The shapes of the small hole Fermi surface around the $\bar{X}$ point and one electron Fermi surface around the $\bar{\Gamma}$ point are generally consistent with the band calculation. In the PEAD pattern, however, there are some photoemission intensities which deviate from the band calculation being consistent with the results of the conventional ARPES measurement. In order to investigate the Fermi surface shape more accurately, however, it is desired to perform the measurement in higher angular and energy resolutions. By comparing the observed PEAD patterns with the simulated ADAO pattern, the symmetry of the atomic orbital composing the Fermi surface of Sr_2RuO_4 is qualitatively determined as d_{xy}, d_{yz} and d_{zx}-like in contrast to that of the HTSC which is $d_{x^2-y^2}$-like orbital. This result is consistent with the prediction of the band calculations. Our observed PEAD patterns of Fermi surface have also indicated the possible existence of the extended van Hove singularity which has been suggested by the conventional high resolution ARPES measurement.

Acknowledgements

We are much obliged to the staff of the machine group of the SRL-ISSP. This study was supported by a Grant in Aid for Specially Promoted Research from the Ministry of Education, Science, Sports and Culture, Japan. This work was carried out by the joint research in the Institute for Solid State Physics, the University of Tokyo.

1) Y. Maeno, H. Hashimoto, K. Yoshida, S. Nishizaki, T. Fujita, J. G. Bednorz and F. Lichtenberg: Nature **372** (1994) 532.
2) R. J. Cava, B. Batlogg, K. Kiyono, H. Takagi, J. J. Krajewski, W. F. Peck, Jr., L. W. Rupp, Jr. and C. H. Chen: Phys. Rev. B **49** (1994) 11890.
3) T. Oguchi: Phys. Rev. B **51** (1995) 1385.
4) D. J. Singh: Phys. Rev. B **52** (1995) 1358.
5) T. Yokoya, A. Chainani, T. Takahashi, H. Katayama-Yoshida, M. Kasai and Y. Tokura: Phys. Rev. Lett. **76** (1996) 3009; T. Yokoya, A. Chainani, T. Takahashi, H. Ding, J. C. Campuzano, H. Katayama-Yoshida, M. Kasai and Y. Tokura: Phys. Rev. B **54** (1996) 13311.
6) D. H. Lu, M. Schmidt, T. R. Cummins, S. Schuppler, F. Lichtenberg and J. G. Bednorz: Phys. Rev. Lett. **76** (1996) 4845.
7) A. P. Mackenzie, S. R. Julian, A. J. Diver, G. J. McMullan, M. P. Ray, G. G. Lonzarich, Y. Maeno, S. Nishizaki and T. Fujita: Phys. Rev. Lett. **76** (1996) 3786.
8) H. Daimon: Rev. Sci. Instrum. **59** (1988) 545; H. Nishimoto, H. Daimon, S. Suga, Y. Tezuka, S. Ino, I. Kato, F. Zenitani and H. Soezima: *ibid.* **64** (1993) 2857.
9) M. Schmidt, T. R. Cummins, M. Bürk, D. H. Lu, N. Nücker and S. Schuppler: Phys. Rev. B **53** (1996) 14761.
10) I. H. Inoue, Y. Aiura, Y. Nishihara, Y. Haruyama, S. Nishizaki, Y. Maeno, T. Fujita, J. G. Bednorz and F. Lichtenberg: J. Electron Spectrosc. Relat. Phenom. **78** (1996) 175.
11) H. Daimon, S. Imada, H. Nishimoto and S. Suga: J. Electron Spectrosc. Relat. Phenom. **76** (1995) 487.
12) L. F. Mattheiss: Phys. Rev. Lett. **58** (1987) 1028; J. Yu, A. J. Freeman and J. H. Xu: Phys. Rev. Lett. **58** (1987) 1035.
13) T. Oguchi (private communication).